

Article

Determination of Anchor Drop Sequence during Vessel Anchoring Operations Based on Expert Knowledge Base and Hydrometeorological Conditions

Jakub Wnorowski and Andrzej Lebkowski * 

Department of Ship Automation, Gdynia Maritime University, Poland Morska 83 Str., 81-225 Gdynia, Poland; j.wnorowski@we.umg.edu.pl

* Correspondence: a.lebkowski@we.umg.edu.pl

Abstract: Presently, the most common technique for maintaining a ship's location is dynamic positioning, which uses a series of thrusters to hold its position. This method is resilient to moderate hydro-meteorological conditions, eliminating the need for extensive preliminary steps before initiating positioning operations. An alternative approach involves station keeping using a set of anchors, where thrusters are not employed, necessitating careful planning of the anchorage in light of hydro-meteorological conditions. Presently, in vessels using this anchoring method, the captain determines the order of anchor drops, taking into account the prevailing weather conditions, the ship's maneuvering abilities, and vessel capability plots. This article introduces a novel algorithm that uses sensor-acquired weather data and a cognitive knowledge base to establish the best sequence for anchor drops. This innovation represents a significant stride towards the automation of the anchoring process. By using the anchorage planning algorithm presented in this publication, it has been possible to reduce the time required for anchor deployment by about 52%, due to the preparation of the anchor deployment strategy in port. A reduction in energy consumption of about 8% was also achieved.

Keywords: anchorage planning; anchor-based positioning system; Unity3D; cognitive knowledge base



Citation: Wnorowski, J.; Lebkowski, A. Determination of Anchor Drop Sequence during Vessel Anchoring Operations Based on Expert Knowledge Base and Hydrometeorological Conditions. *Electronics* **2024**, *13*, 176. <https://doi.org/10.3390/electronics13010176>

Academic Editors: Mahmut Reyhanoglu, Erkan Kayacan and Mohammad Jafari

Received: 20 November 2023
Revised: 22 December 2023
Accepted: 29 December 2023
Published: 30 December 2023



Copyright: © 2023 by the authors. Licensee MDPI, Basel, Switzerland. This article is an open access article distributed under the terms and conditions of the Creative Commons Attribution (CC BY) license (<https://creativecommons.org/licenses/by/4.0/>).

1. Introduction

With advances in technology, the maritime industry has seen an increased demand for specialized vessels capable of holding a designated position for extended periods of time. Such vessels can perform a variety of functions, including oil exploration [1,2], performing salvage operations, laying pipelines [3,4], conducting seismic surveys [5] or operating wind farms [6]. In many applications, for example in ROVs [7], the preferred positioning system is dynamic positioning, using a set of thrusters to maintain the vessel's position. Currently, global researchers are focusing on the research and development of components related to dynamic positioning, as evidenced by the significant number of publications on the subject, including those related to control systems [8–11].

Despite the wide applicability and adaptability of dynamic positioning, its economic viability for long-term operations of at least one day may be questionable due to the continuous energy and fuel consumption. In such scenarios, a positioning system based on a set of anchors may be a more efficient alternative. In this approach, symmetrically placed anchors around the vessel, as shown in Figure 1, are used to hold the vessel's position instead of thrusters. This configuration allows unlimited changes in the vessel's position in any direction.

In the case of positioning using a set of anchors, a crucial aspect involves the planning of the anchorage area and determining the sequence of anchor deployment. This is significant due to the limited maneuverability and less powerful thrusters of such vessels, unlike ships equipped with dynamic positioning. Improperly designed anchorage areas

may result in the inability to deploy all anchors, leading to delays in crew operations. Currently, there is a lack of literature and publications focused on anchorage planning from the perspective of positioning systems, as opposed to publications related to ship route planning [12–18] or precise maneuvering [19–21]. Existing publications related to anchorages often pertain to ships awaiting anchorage outside ports, as in the publication [22], where the authors present an anchorage planning algorithm in the presence of other anchored vessels. Other publications, such as [23–27], concentrate on algorithms for determining berthing locations for vessels dropping anchors.

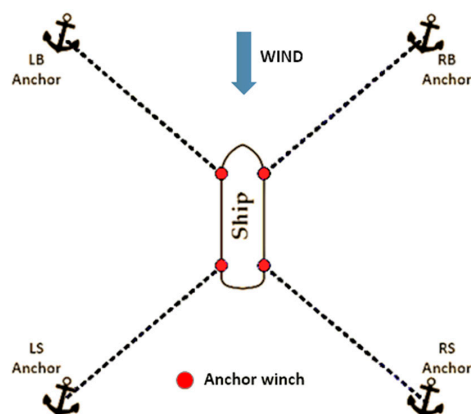


Figure 1. Example of anchor arrangement.

This publication introduces a new approach to anchorage planning based on the utilization of cognitive knowledge. Cognitive knowledge, in this context, refers to a set of rules developed from expert knowledge. Through the application of cognitive knowledge, the anchorage planning process can be automated, limiting the human factor to defining the expected hydrometeorological conditions in the anchor deployment area. These rules have been formulated based on charts depicting position-keeping capabilities (capability plots), information about the vessel’s maneuverability (detailed in the subsequent sections of the paper), and the outcomes of conducted research. This paper also presents a step-by-step walkthrough of the entire anchorage planning process using a tool developed in the Unity3D environment.

2. The Mathematical Models and Research Methodology

In order to develop a cognitive knowledge base for designing anchorage elements, such as optimal anchor deployment locations around the positioning operation area or the vessel’s heading relative to the wind direction, the first step is to obtain information regarding the ship’s behavior under environmental forces. Analyzing the ship’s behavior in hydrometeorological conditions involves creating so-called position-keeping capability charts for the vessel. Information about the thrusters employed and their parameters can be found in the technical documentation of the ship. The data used for analysis include the type, power, and maximum thrust of each thruster.

Subsequently, based on the gathered data, decision-making rules can be formulated to serve as the foundation for the cognitive knowledge base. These rules should account for interactions between environmental forces and the vessel, as well as consider thruster parameters. The cognitive knowledge base can be utilized to automate the anchorage planning process, enabling effective responses to changing sea conditions.

2.1. The Technical Specifications of the Vessel

The analysis of position-keeping capabilities begins with defining parameters such as the dimensions of the vessel, surfaces, and information about the thrusters. Table 1 presents basic data concerning the vessel on which the research was conducted to develop the cognitive knowledge base.

Table 1. The parameters of the considered vessel.

| Parameter | Value |
|---|-------|
| Length overall (L_{oa}) [m]: | 72.7 |
| Length between perpendiculars (L_{pp}) [m]: | 64 |
| Breadth [m]: | 11.6 |
| Draught [m]: | 3.4 |
| Displacement [T]: | 1886 |
| Distance between foremost and aft most point of the hull below the surface at design draft even keel [m]: | 67.1 |
| Water plane area [m ²]: | 639 |
| Projected longitudinal area above water [m ²]: | 437 |
| Surge position of geometric center of the projected longitudinal area above water with respect to $L_{pp}/2$ [m]: | 0.1 |
| Projected longitudinal area below water [m ²]: | 223 |
| Surge position of geometric center of the projected longitudinal area below water with respect to $L_{pp}/2$ [m]: | −2.9 |
| Surge position of water line center with respect to $L_{pp}/2$ [m]: | −1.5 |
| Projected transverse area above water [m ²]: | 140 |
| Projected transverse area below water [m ²]: | 36 |

The vessel is equipped with 4 thrusters, including 2 tunnel thrusters and 2 main propellers. Data regarding each thruster and their positions relative to the $L_{pp}/2$ point are presented in Table 2 and Figure 2.

Table 2. The maximum thrust values for individual thrusters.

| Thruster | Thrust Max [kN] | Thrust Min [kN] | Power [kW] |
|----------------|-----------------|-----------------|------------|
| Tunnel 1 | 94 | −94 | 447 |
| Tunnel 2 | 94 | −94 | 447 |
| Port propeller | 179 | −179 | 2000 |
| Stbd propeller | 179 | −179 | 2000 |

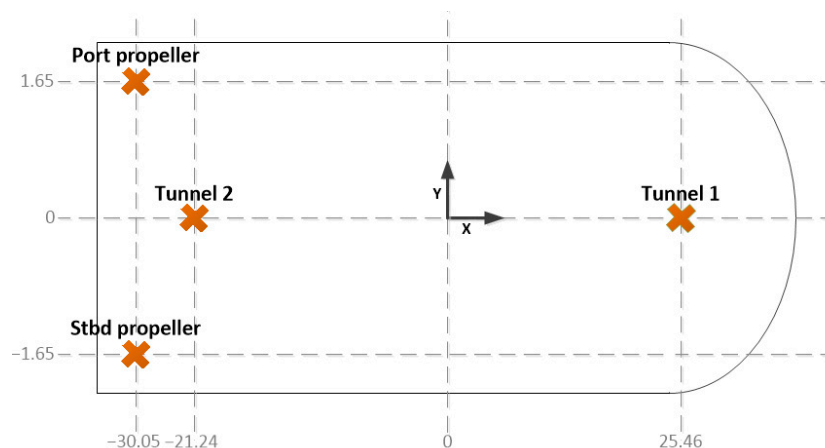


Figure 2. The arrangement of thrusters on the ship.

In the first chapter, it was mentioned that ships equipped with a positioning system based on a set of anchors usually do not have thrusters with sufficient power to keep their position. These thrusters serve only to move between individual anchor deployment points.

In addition to the mentioned thrusters, the unit is equipped with 4 anchor winches—two at the bow and two at the stern. Table 3 provides information on the maximum

tension of anchor ropes corresponding to three example lengths of the deployed rope, while Figure 3 illustrates the positions of individual anchor winches on the ship.

Table 3. The maximum pull of the anchor winch corresponding to the length of the deployed rope.

| Winch | Max Pull [kN] (500 m Rope) | Max Pull [kN] (750 m Rope) | Max Pull [kN] (1000 m Rope) |
|-------|-------------------------------|-------------------------------|--------------------------------|
| LB | 102.53 | 116.47 | 124.85 |
| RB | 102.53 | 116.47 | 124.85 |
| LS | 102.53 | 116.47 | 124.85 |
| RS | 102.53 | 116.47 | 124.85 |

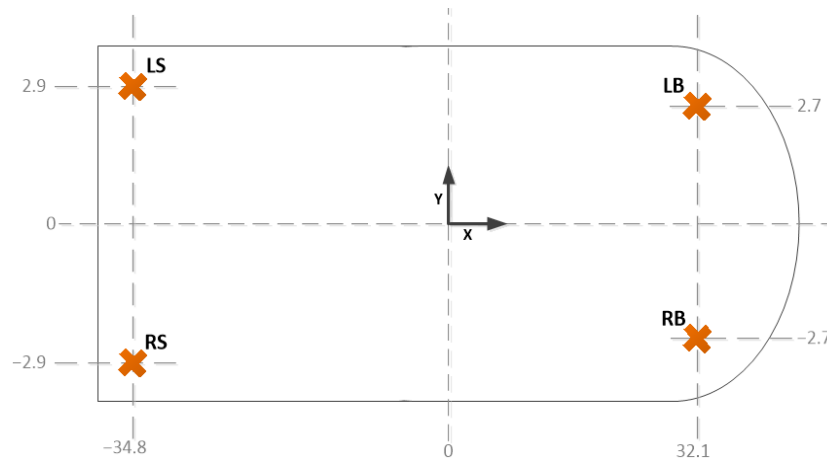


Figure 3. The arrangement of anchor winches on the ship.

In creating capability plots for the vessel, it is essential to consider the difference in maximum tension force based on the length of the deployed anchor rope.

2.2. Capability Plots

The capability plots for the vessel depict the results of an analysis on the impact of environmental forces on station keeping. Figure 4 illustrates a sample chart, which consist of three layers:

- The shape located at the center of the chart represents the silhouette of the vessel;
- The numbers located on the outer periphery represent the angle of attack of environmental forces on the ship’s hull;
- The green line delineates the maximum wind speed value (in knots) that can exert an effect on the ship’s hull at a given angle while keeping the target position.

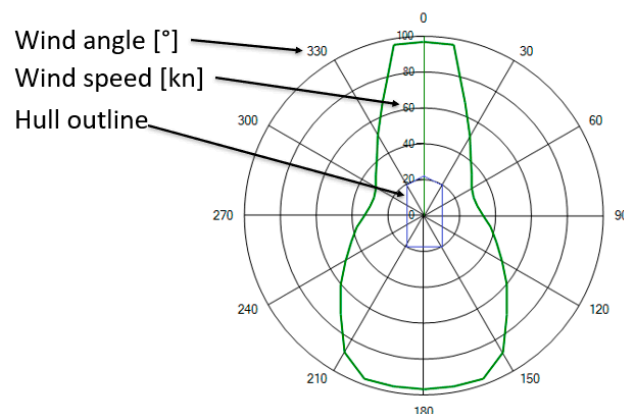


Figure 4. An exemplary chart illustrating the position-keeping capability of the vessel.

The determination of the characteristic depicted in Figure 4 begins with defining the model of environmental forces acting on the ship's hull. These environmental forces are categorized into three groups:

- Wind force and torque;
- Sea current force and torque;
- Sea waves force and torque.

2.2.1. Wind Force and Torque

The mathematical model of the wind acting on the vessel consists of three equations that determine the distribution of wind force along the X and Y axes of the ship, as well as the Yaw moment [28]. It is assumed that the wind always acts on the point $L_{pp}/2$ of the ship (L_{pp} —Length Between Perpendiculars).

$$X_w = q \cdot K_X(\theta_w) \cdot A_{FW} \quad (1)$$

$$Y_w = q \cdot K_Y(\theta_w) \cdot A_{LW} \quad (2)$$

$$M_w = q \cdot K_M(\theta_w) \cdot A_{FW} \cdot H_{FW} \quad (3)$$

where: θ_w —the wind angle relative to the point $L_{pp}/2$ [°]; q —wind pressure on the ship's hull factor; K_X —shape coefficient for the x-axis [-]; A_{FW} —cross-sectional area of the above-water part of the hull [m²]; K_Y —shape coefficient for the y-axis [-]; A_{LW} —side area of the hull above the waterline [m²]; K_M —shape coefficient of the hull for the torsional moment [-]; H_{FW} —displacement of the geometric center of the above-water side area of the hull relative to the point $L_{pp}/2$ [m].

The hull shape coefficients (K_X , K_Y , and K_M) were determined based on the publication [28]:

$$K_X(\theta_w) = -CD_l \cdot \frac{A_{LW}}{A_{FW}} \cdot \frac{\cos(\theta_w)}{1 - \frac{\delta}{2} \cdot \left(1 - \frac{CD_l}{CD_t}\right) \cdot \sin^2(2 \cdot \theta_w)} \quad (4)$$

$$K_Y(\theta_w) = CD_t \cdot \frac{\sin(\theta_w)}{1 - \frac{\delta}{2} \cdot \left(1 - \frac{CD_l}{CD_t}\right) \cdot \sin^2(2 \cdot \theta_w)} \quad (5)$$

$$K_M(\theta_w) = k \cdot K_Y(\theta_w) \quad (6)$$

where: CD_l —longitudinal resistance coefficient [-]; CD_t —lateral resistance coefficient [-]; δ —cross-force coefficient [-]; k —rolling moment coefficient [-].

The values of CD_l and CD_t depend on the type of vessel. For the above example, it was assumed that $CD_l \in [0.55, 0.65]$, $CD_t = 0.9$, $k = 1.2$, $\delta = 0.55$.

The individual values of K_X , K_Y , and K_M are presented in Figure 5.

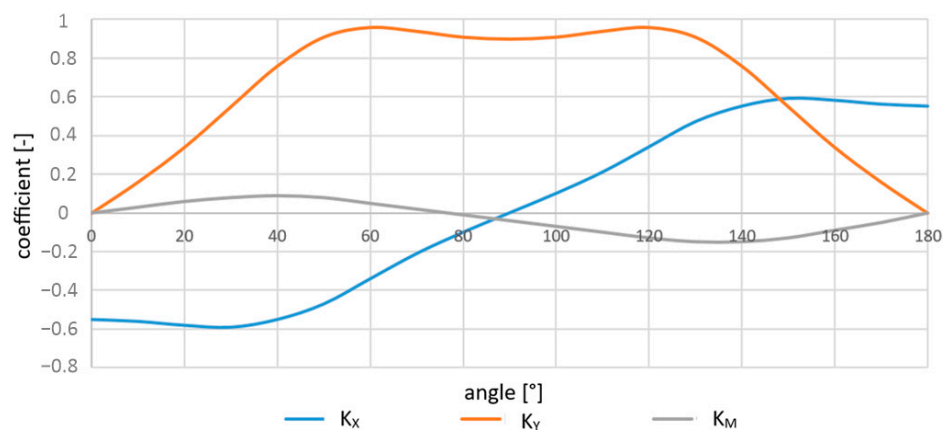


Figure 5. Ship shape coefficients.

The factor determining the wind pressure on the ship’s hull is shown by the following function

$$q = \frac{1}{2} \cdot \rho_a \cdot V_w^2 \tag{7}$$

where: ρ_a —air density [kg/m³]; V_w —wind speed [m/s].

2.2.2. Sea Current Force and Torque

Forces originating from the sea current and its Yaw moment are determined analogously to the wind force (Equations (1)–(3)). In this case, unlike the wind force, surfaces located beneath the waterline are taken into account.

$$X_c = q_c \cdot K_X(\theta_C) \cdot A_{FC} \tag{8}$$

$$Y_c = q_c \cdot K_Y(\theta_C) \cdot A_{LC} \tag{9}$$

$$M_c = q_c \cdot K_M(\theta_C) \cdot A_{FC} \cdot H_{FC} \tag{10}$$

where: θ_C —the angle of the sea current relative to the point $L_{pp}/2$ [°]; q_c —sea current pressure on the ship’s hull factor; K_X —shape coefficient for the x -axis [-]; A_{FC} —cross-sectional area of the underwater part of the hull [m²]; K_Y —shape coefficient for the y -axis [-]; A_{LC} —side area of the hull below the waterline [m²]; H_{FC} —displacement of the geometric center of the underwater side area of the hull relative to the point $L_{pp}/2$ [m].

The factor determining the sea current pressure on the ship’s hull is shown by the following function

$$q = \frac{1}{2} \cdot \rho_c \cdot V_c^2 \tag{11}$$

where: ρ_c —air density [kg/m³]; V_c —sea current speed [m/s].

2.2.3. Sea Waves Force and Torque

The mathematical model of ocean waves that affect the ship’s hull depends on the utilized wave spectrum. In the literature, for example [29], two are most commonly employed: JONSWAP and the Pierson–Moskowitz spectrum [30]. The classification society DNV (Det Norske Veritas) [31], in their documents concerning the analysis of a ship’s position-keeping capabilities, applies the Moskowitz spectrum. Below is a mathematical model enabling the determination of individual components of ocean wave forces acting on the ship’s hull. The model comes from the document titled “Assessment of station keeping capability of dynamic positioning vessels”, which is available on the DNV website [32].

$$X_{waves} = q \cdot B \cdot h(Dir, bow_a, C_{WLaft}) \cdot f(T'_s) \tag{12}$$

$$h(Dir, bow_a, C_{WLaft}) = 0.09 \cdot h_1(Dir, bow_a, C_{WLaft}) \cdot h_2(Dir) \tag{13}$$

$$h_{1A}(bow_a) = 0.8 \cdot bow_a^{4.5} \tag{14}$$

$$h_{1B}(C_{WLaft}) = 0.7 \cdot C_{WLaft}^2, C_{WLaft} \in [0.85, 1.15] \tag{15}$$

$$dir(Dir) = \begin{cases} Dir, & 0 \leq Dir \leq \pi \\ 2\pi - Dir, & \pi \leq Dir \leq 2\pi \end{cases} \tag{16}$$

$$h_1(Dir, bow_a, C_{WLaft}) = h_{1A}(bow_a) + \frac{dir(Dir)}{\pi} (h_{1B}(C_{WLaft}) - h_{1A}(bow_a)) \tag{17}$$

$$h_2(Dir) = 0.05 + 0.95 \cdot \tan^{-1}(1.45 \cdot (dir(Dir) - 1.75)) \tag{18}$$

$$f(t') = \begin{cases} 1, & \text{if } t' < 1 \\ t'^{-3} \cdot e^{1-t'^{-3}}, & \text{if } t' \end{cases} \tag{19}$$

$$Y_{waves} = q \cdot L_{OS} \cdot (0.09 \cdot \sin(Dir)) \cdot f(T'_{sw}) \quad (20)$$

$$M_{waves} = Y_{waves} \cdot \left(X_{Los} + \left(0.05 - 0.14 \cdot \frac{dir(Dir)}{\pi} \right) \right) \cdot L_{OS} \quad (21)$$

$$T'_s = \frac{T_z}{0.9 \cdot L_{pp}^{0.33}} \quad (22)$$

$$T'_{sw} = \frac{T_z}{0.75 \cdot B^{0.5}} \quad (23)$$

$$H_s = 0.3125 \cdot V_w - 0.62 \quad (24)$$

$$T_z = 0.741 \cdot V_w + 0.536 \quad (25)$$

where: B —maximum breadth at water line [m]; Dir —waves coming from direction [$^\circ$]; bow_a —angle between the vessel x -axis and a line drawn foremost point in the water line to the point at $y = B/4$ on the water line [$^\circ$]; C_{WLft} —water plane area coefficient of the water plane area behind midship [-]; L_{os} —longitudinal distance between the fore most and aft most point under water [m]; X_{Los} —longitudinal position of $L_{os}/2$ [m]; L_{pp} —length between perpendiculars [m]; H_s —significant wave height [m]; A_{WLft} —water plane area for $x < 0$ [m²];

2.2.4. The Mathematical Model of Anchor Winch Forces

The next step after defining the mathematical model of environmental forces acting on the hull is to define the mathematical model of elements to keep the vessel at the target position. In the case of dynamic positioning, these elements are thrusters, while in the scenario described in this paper, they are anchor windlasses. For the purpose of illustrating the algorithm used to plan the anchorage, it is assumed that the mathematical model of forces generated by anchor windlasses along each axis of the ship will be as follows:

$$X_{Force} = F_W \cdot \cos\alpha \quad (26)$$

$$Y_{Force} = F_W \cdot \sin\alpha \quad (27)$$

$$M = F_W (\sin\alpha \cdot Pos_X) (\cos\alpha \cdot Pos_Y) \quad (28)$$

where: X_{Force} —force generated by the anchor winch acting on the x -axis of the ship [kN]; α —Angle between the anchor winch and the deployed anchor [$^\circ$]; Y_{Force} —force generated by the anchor winch acting on the y -axis of the ship [kN]; M —torsional moment generated by the anchor winch; F_W —maximum pull force of the anchor winch [kN]; Pos_X —position of the anchor winch on the x -axis relative to the point $L_{pp}/2$ [m]; Pos_Y —position of the anchor winch on the y -axis relative to the point $L_{pp}/2$ [m];

With the mathematical models of environmental forces and anchor winches defined, the next step is to solve the system of equations comprising Equations (29)–(39) to find the minimum respective tension values for the anchor winches to keep the vessel at the target position. For Equations (29)–(39), it is assumed that the modeled vessel is equipped with 4 anchor winches—2 located at the bow of the ship and 2 at the stern. The following designations for the anchor winches are assumed:

- LB—left bow anchor winch;
- RB—right bow anchor winch;
- LS—left stern anchor winch;
- RS—right stern anchor winch.

$$X_{Force_{LB}} + X_{Force_{RB}} + X_{Force_{LS}} + X_{Force_{RS}} = -(X_w + X_c + X_{waves}) \quad (29)$$

$$Y_{Force_{LB}} + Y_{Force_{RB}} + Y_{Force_{LS}} + Y_{Force_{RS}} = -(Y_w + Y_c + Y_{waves}) \quad (30)$$

$$M_{Force_{LB}} + M_{Force_{RB}} + M_{Force_{LS}} + M_{Force_{RS}} = -(M_w + M_c + M_{waves}) \quad (31)$$

$$F_{WLB} \geq 0 \text{ AND } F_{WLB} < \text{max_tension} \quad (32)$$

$$\alpha_{LB} \geq 300^\circ \text{ AND } \alpha_{LB} \leq 330^\circ \quad (33)$$

$$F_{WRB} \geq 0 \text{ AND } F_{WRB} < \text{max_tension} \quad (34)$$

$$\alpha_{RB} \geq 30^\circ \text{ AND } \alpha_{RB} \leq 60^\circ \quad (35)$$

$$F_{WLS} \geq 0 \text{ AND } F_{WLS} < \text{max_tension} \quad (36)$$

$$\alpha_{LS} \geq 210^\circ \text{ AND } \alpha_{LS} \leq 240^\circ \quad (37)$$

$$F_{WRS} \geq 0 \text{ AND } F_{WRS} < \text{max_tension} \quad (38)$$

$$\alpha_{RS} \geq 120^\circ \text{ AND } \alpha_{RS} \leq 150^\circ \quad (39)$$

where: $X_{Force_{LB}}, X_{Force_{RB}}, X_{Force_{LS}}, X_{Force_{RS}}$ —tension forces of anchor ropes acting on the x -axis of the ship, originating from the anchor winches; $Y_{Force_{LB}}, Y_{Force_{RB}}, Y_{Force_{LS}}, Y_{Force_{RS}}$ —tension forces of anchor ropes acting on the y -axis of the ship, originating from the anchor winches; $M_{Force_{LB}}, M_{Force_{RB}}, M_{Force_{LS}}, M_{Force_{RS}}$ —torsional moment generated by individual anchor winches; $F_{WLB}, F_{WRB}, F_{WLS}, F_{WRS}$ —the tension forces of each anchor winch that need to be determined; $\alpha_{LB}, \alpha_{RB}, \alpha_{LS}, \alpha_{RS}$ —the angle between the anchor winch and the anchor.

To determine the individual values of the tension forces, we utilized the Ipopt library (Interior Point Optimizer) and the MUMPS solver (MULTifrontal Massively Parallel sparse direct Solver). The aforementioned solver allows for finding a solution in cases of fewer equations, as it operates on the principle of substituting values into the equations and checking if all conditions are met. The operation of the solver can be described as follows:

1. Based on the constraints, determine initial values, and then substitute them into the system of equations.
2. Check if the obtained values of the tension of each anchor winch are able to balance the given environmental forces. If not, determine a new set of values, substitute them into the equations, and recheck the solution. Repeat until a solution is found.

The algorithm for determining capability plots aims to find the appropriate distribution of thrust forces for the thrusters (in the case of DP systems) or tension of the anchor ropes (in the case of an anchor-based system) to resist the environmental forces acting on the vessel. The operation of the algorithm is as follows:

1. Set the wind angle to 0° .
2. Set the wind speed to 25 m/s and the current speed to 0.75 m/s (according to DNV guidelines).
3. Calculate the environmental force value for the specified wind speed.
4. Find the thrust allocation on the thrusters (or the tension in the anchor ropes) capable of resist the environmental forces.
5. If a suitable force distribution capable of counteracting environmental forces is found, increase the wind speed and repeat steps 3–5. If not, decrease the wind speed and repeat steps 3–5.
6. Repeat step 5 until the maximum wind speed at which the vessel can keep its position at a given wind angle is obtained. Add the point with the maximum wind value and current angle to the polar plot.
7. Once the maximum wind speed for a given angle has been determined, increase the wind angle by 10° . Repeat steps 2–6.

3. Anchorage Planning Using Cognitive Knowledge Base

The process of anchorage planning should commence with defining rules within the cognitive knowledge base, enabling the automation of the anchoring deploy process. These rules have been implemented in a tool developed in the Unity3D environment, designed for anchorage planning.

3.1. Cognitive Knowledge Base

The cognitive knowledge base consists of a set of rules that can be developed based on expert knowledge or through conducted analyses, tests, and experiments. The rules have been categorized into the following sections:

- Rules related to an optimal anchor deployment field, such as:

*IF (depth == 15 m AND anchor LB == SELECTED) THEN
(show anchor deployment field for anchor LB) AND
(set the maximum anchor deployment distance to 1000 m – depth)*

*IF (anchor LB == SELECTED) THEN
(the initial angle between the anchor winch LB and anchor LB can be $315^\circ \pm 25^\circ$)*

- Rules related to the selection of the ship's course, for example:

*IF (wind angle of attack on the hull == 90°) THEN
(set the proposed course of the ship to 90° or 270°)*

- Rules related to the selection of the anchor deployment location, such as:

*IF (ship movement along the x-axis == ± 20 m) THEN
(set the distance of anchor LB and RB from the ship at 35 m + a constant value) AND
(set the angle between anchor winch LB and anchor LB to 330°) AND
(set the angle between anchor winch RB and anchor RB to 30°)*

Sample pseudocode of the algorithm implementing the rule:

*IF (depth == 15 m AND anchor LB == SELECTED) THEN
(show anchor deployment field for anchor LB) AND
(set the maximum anchor deployment distance to 1000 m – depth)*

looks like follows (Algorithm 1):

Algorithm 1: CheckDepthValue

BEGIN

- 1: if DepthText.text == "" or DepthText.text == null then set DepthText.text as 0
- 2: if Anchor_LB == used then calculate new anchoring area and set the maximum anchor deployment distance to 1000 – float.Parse(DepthText.text)
- 3: if Anchor_RB == used then calculate new anchoring area and set the maximum anchor deployment distance to 1000 – float.Parse(DepthText.text)
- 4: if Anchor_LS == used then calculate new anchoring area and set the maximum anchor deployment distance to 1000 – float.Parse(DepthText.text)
- 5: if Anchor_RS == used then calculate new anchoring area and set the maximum anchor deployment distance to 1000 – float.Parse(DepthText.text)

END

CheckDepthValue()

To implement the algorithm presented in this publication on the ship, the rules for the anchor deployment process were integrated into the cognitive knowledge base. Throughout the operation, the algorithm dynamically assesses the ongoing anchor deployment stage, adjusting the rules accordingly. The various stages of anchor deployment, with concise examples of the associated rules, are described as follows:

Stage 1: Loading the planned anchorage into the ship's control system in the form of waypoints.

Stage 2: Set the course for the first anchor and adjust the declared speed.

IF (ship course != target course) THEN
(adjust the rudder to achieve the desired course)
IF (ship speed != target speed) THEN
(increase the main propeller RPMs to achieve the desired speed)

Stage 3: Stop the vessel at the designated drop point for the first anchor.

IF (ship position == first anchor position \pm 5 m) THEN
(stop engines and keep position)

Stage 4: Begin to slacken the anchor rope until it touches the seabed.

IF (anchor line tension > 0) THEN
(anchor has not touched seabed. Loosen the anchor rope)

On the ship, the anchor winches operators followed the rule that the length of anchor rope should be twice the depth. Therefore, a similar rule can be applied:

*IF (anchor rope length < 2*depth) THEN*
(anchor has not touched seabed. Loosen the anchor rope)

Stage 5: When the tension of the anchor line reaches 0 or the appropriate length of the anchor rope has been released, begin to move slowly towards the next anchor. At this stage, it is crucial to observe whether the tension of the anchor rope is increasing. If not, it indicates that the anchor has not successfully engaged the seabed. In such a scenario, the vessel should be maneuvered directly over the anchor (positioning the ship precisely above the anchor) and pull in it. Subsequently, repeat stage 4:

IF (anchor line tension > 2 kN) THEN
<(adjust the rudder to achieve the course for next anchor) AND
(increase the main propeller RPMs to achieve the desired speed)

IF (anchor line tension < 2 kN) THEN
(return to the anchor drop point) AND
(pull in the anchor) AND
(return to stage 4)

Stages 1 to 5 should be repeated for each subsequent anchor.

Stage 6: At this point, all anchors have been dropped. The ship should be moved to the target point.

IF (anchor LB == dropped) AND
(anchor RB == dropped) AND
(anchor LS == dropped) AND
(anchor RS == dropped) THEN
(turn off main engine) AND
<pull in the anchor ropes until the ship is at the desired point>

At each of the above stages, it may turn out that environmental conditions differ from those declared during anchorage planning. In such a case, based on the anchors already deployed, the algorithm will suggest modifications to the anchorage.

In developing the rules, charts depicting the vessel's position-keeping capabilities were utilized, providing insights into the impact of environmental conditions on the specified position. In the described scenario, three analyses were conducted, following the data from Table 3. These analyses have enriched the cognitive knowledge base with additional rules and data crucial for anchorage planning. The results of these analyses are presented in Figure 6

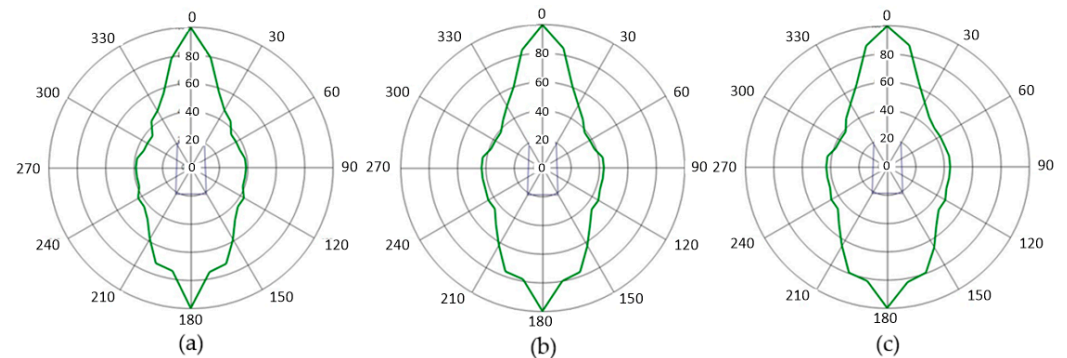


Figure 6. Capability plots for 3 values of maximum anchor rope tension: (a) For 102.53 kN (500 m); (b) For 116.47 kN (750 m); (c) For 124.85 kN (1000 m).

From the results of the analyses presented in Figure 6, it can be observed that in each scenario, the vessel is capable of keeping its position with wind speeds reaching up to 100 knots (approximately 50 m/s), provided that the wind acts on the ship at an angle of 0° or 180° . This is attributed to the streamlined shape of the vessel. As the angle of wind influence increases, the surface area increases, reducing the position-keeping capability. At a wind angle of 60° or 300° , the maximum wind speed at which the ship will maintain its position is: for case (a)—approximately 37 knots, for case (b)—about 40 knots, and for case (c)—42 knots

Constant values were also adopted for the development of rules. The selected values are presented in Table 4.

Table 4. Selected values used for the development of rules.

| Parameter | Value |
|---|--------------------------|
| Initial angle between anchor winch LB and anchor LB | $315^\circ \pm 25^\circ$ |
| Initial angle between anchor winch RB and anchor RB | $45^\circ \pm 25^\circ$ |
| Initial angle between anchor winch LS and anchor LS | $225^\circ \pm 35^\circ$ |
| Initial angle between anchor winch RS and anchor RS | $135^\circ \pm 35^\circ$ |
| Maximum length of the deployed anchor rope [m] | 1000 |
| Minimum length of the deployed anchor rope [m] | 100 |
| Fuel consumption at 100% main engine load [l/h] | 246 |
| Fuel consumption at 100% tunnel thruster load [l/h] | 37 |

3.2. Anchorage Planning in Unity3D

Anchorage planning has been implemented in a tool developed in the Unity3D environment. The main window of the program is presented in Figure 7.

The main window consists of 4 primary elements:

1. Panel for setting anchorage parameters,
2. Indicator of the current course of the ship,
3. Navigation tools on the map, such as zoom in/out, handling the geographic grid, and switching to a mode allowing save picture of the planned anchorage,
4. Geographic grid and bathymetric map.

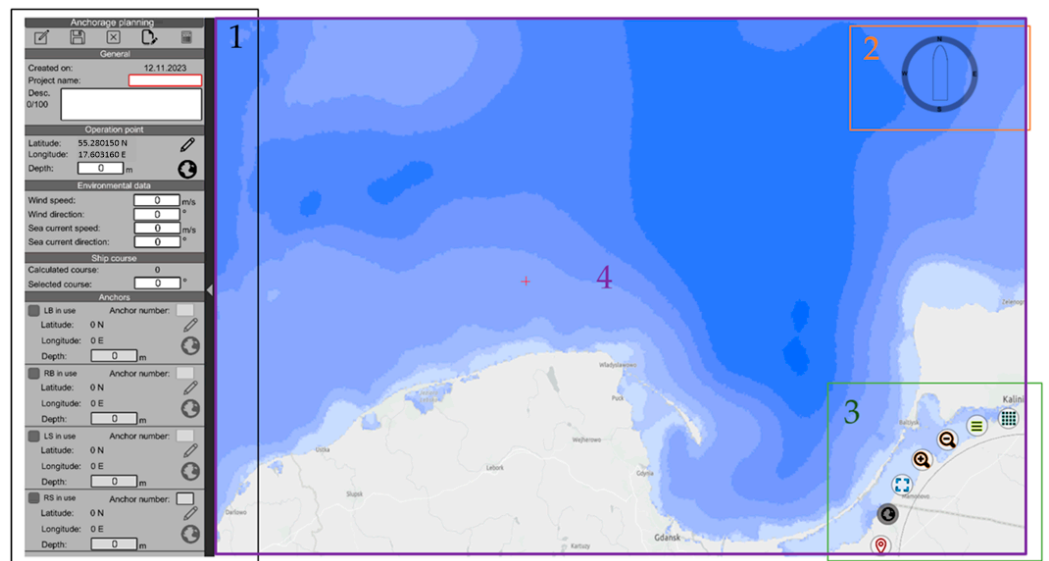


Figure 7. Main window of the anchorage planning tool.

The software allows for downloading maps from a selected bathymetric data provider to obtain information about water depths. It is also possible to upload custom maps in case of no internet connection

The process of anchorage planning begins with defining the point where the ship should be positioned after the anchor deployment process. The target position is defined in the section operation point. Figure 8 presents the placed ship silhouette along with the coordinates. The coordinates were randomly chosen for the purpose of this publication. The water depth will be automatically read from the bathymetric map based on the geographic coordinates.

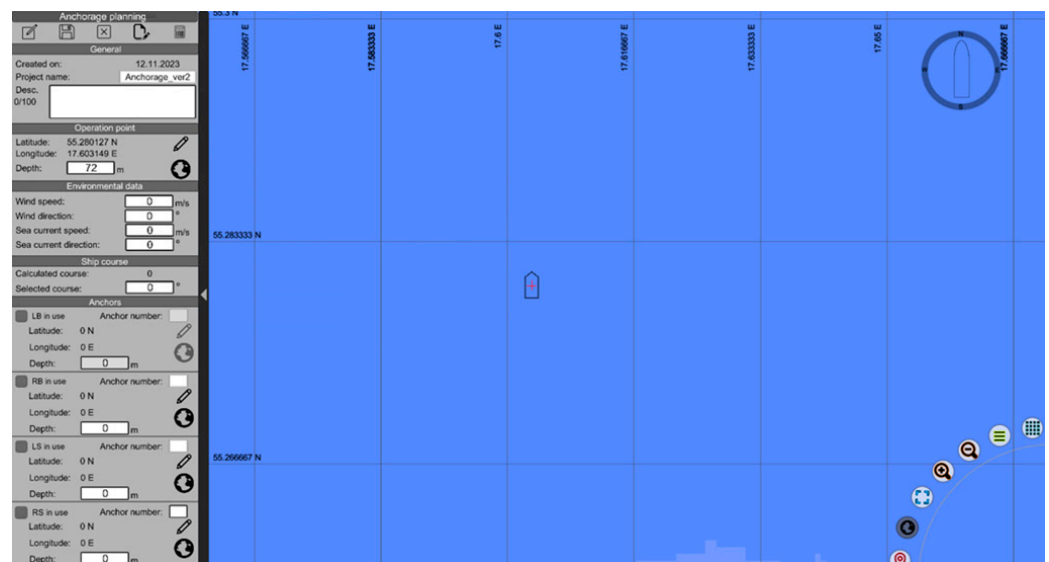


Figure 8. The selected operation position and defined water depth.

The next planning step involves specifying the environmental conditions that the operator expects at the point chosen in the previous step. Example values are presented in Figure 9.

After determining the environmental conditions and the reference point for the ship's positioning, the program suggests a course for the vessel based on information in the cognitive knowledge base. According to the charts of the ship's position-keep capability, the optimal course for the ship should be bow or stern to the wind. However, during

research, it was found that the anchor rope is too heavy, and the tunnel thrusters alone cannot move the ship. Therefore, the algorithm determining the ship's course in this case suggests aligning the ship's side to the wind. This orientation allows for the utilization of environmental forces, which exert the strongest influence on the sides at an angle of 90° or 270° to relieve the tunnel thrusters. Figure 10 shows the silhouette of the ship after the operator has accepted the proposed course.

| Environmental data | |
|------------------------|---------|
| Wind speed: | 5 m/s |
| Wind direction: | 45° |
| Sea current speed: | 0.5 m/s |
| Sea current direction: | 45° |

Figure 9. Expected hydrometeorological conditions during anchoring operations.

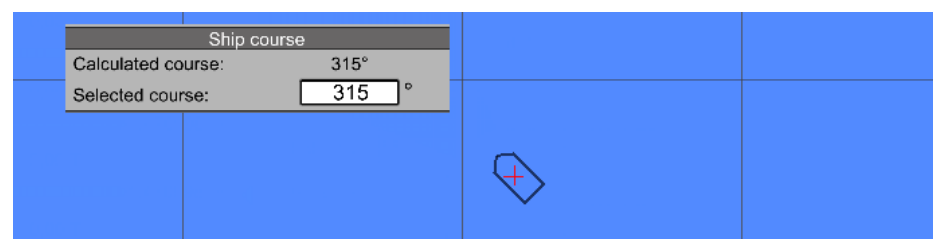


Figure 10. The proposed course for the ship based on the cognitive knowledge base.

In the final step of anchoring planning, locations for dropping individual anchors and the sequence of dropping need to be determined. For this, the number of anchors involved in positioning the ship should be selected. In the case presented in this publication, all 4 anchors will be used, as illustrated in Figure 11.

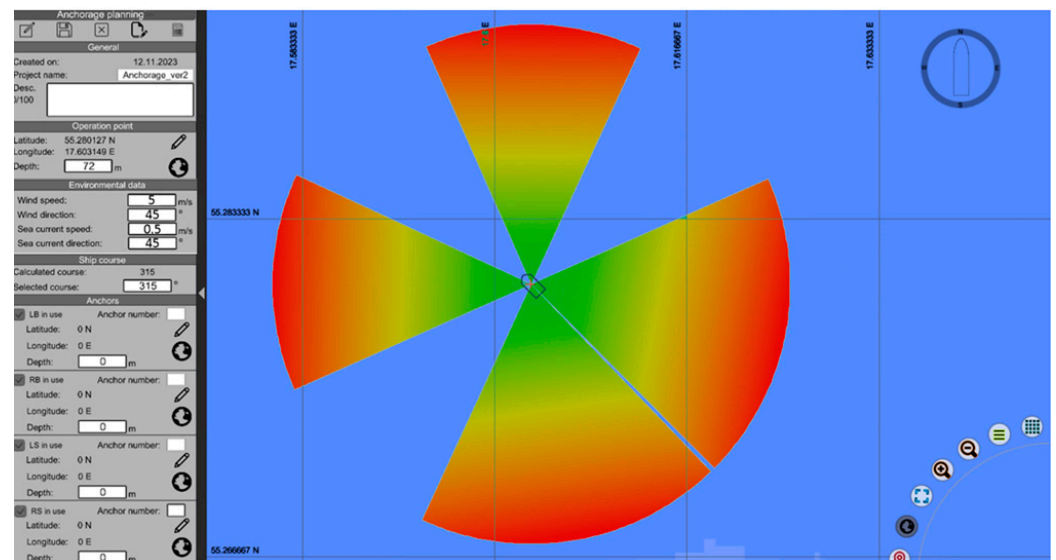


Figure 11. View of the program window after selecting the number of available anchors.

After selecting the anchors that should be available, a field for optimal anchor deployment will appear for each of them. The span of the field has been determined by the rules of the cognitive knowledge base by specifying the angle between the anchor winch and the anchor, as well as the deviation. The maximum distance of anchor deployment from the ship has been limited by the maximum length of the anchor line reduced by the depth value, as derived from trigonometry. Additionally, each optimal anchor deployment zone

is divided into zones determining the theoretical energy consumption needed to deploy the anchor in each location. The green color denotes the smallest value, and the closer to the red color, the greater the value. This division into zones is also associated with determining the stability of maintaining the position. The closer the anchor is deployed to the ship, the smaller its contribution to keeping the position.

The placement of anchors in optimal deployment areas depends on two factors: how much the ship will change its position in the front–back, left–right axes, and the ratio of energy consumption to position stability. To illustrate the maneuverability range, after determining additional coefficients visible in Figure 12, a circle appears, on which anchors will be placed.

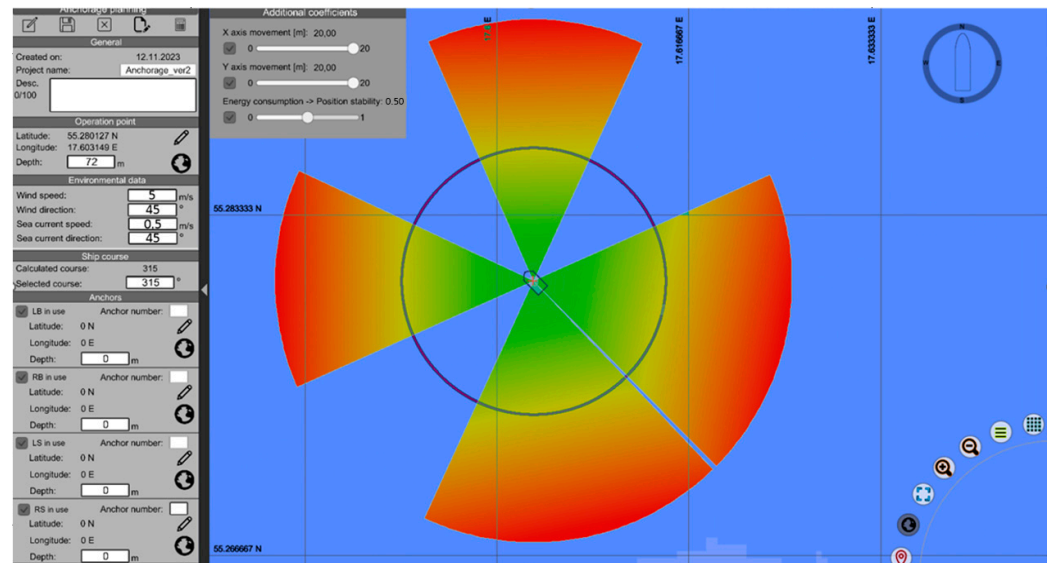


Figure 12. Visualization of the maneuvering area.

Conducting studies under real conditions has shown that the most versatile arrangement of anchors is on the outline of a square. Therefore, for the above configuration, the program will decide on the placement of anchors as presented in Figure 13.

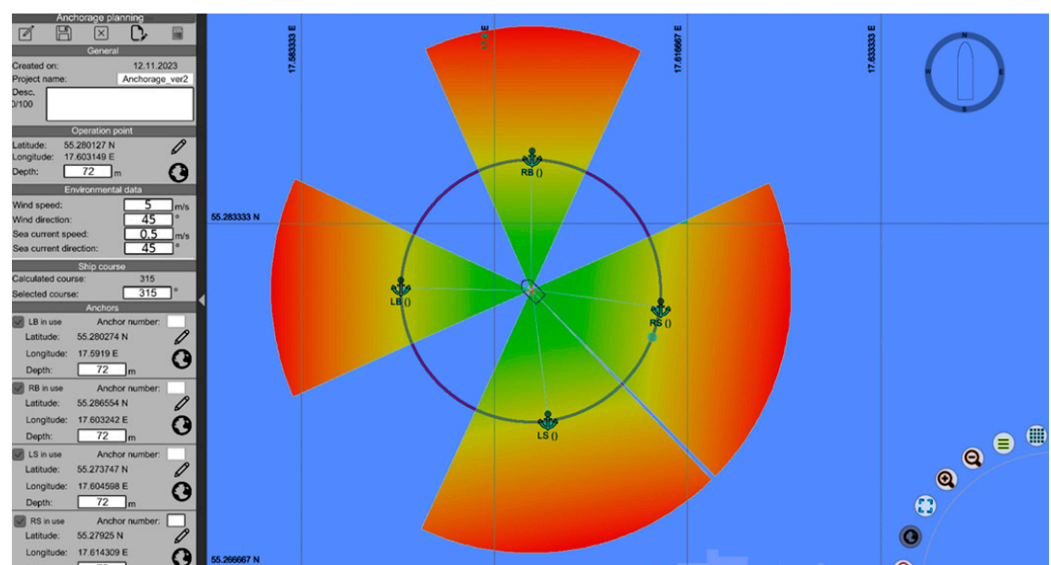


Figure 13. Anchor placement proposed by the algorithm.

The last element is to establish the sequence of dropping individual anchors. During the course determination, it was mentioned that the vessel presented in the publication is

equipped with tunnel thrusters, which do not allow for free movement in the left–right axis when anchors are dropped. To deploy the anchors, the force of the wind must be utilized. Therefore, it is necessary to start deploying the anchors from those on the starboard side. Considering the possible danger of the anchor rope getting entangled in the propulsion screw during forward movement, the program proposed dropping anchor RB first (point 0 on Figure 14). Excluding the possibility of moving forward, the next anchor to be dropped will be anchor LB. The movement of the ship towards anchor LB is indicated by arrow number 1 in Figure 14. With two anchors planned, the algorithm compares the remaining two possible situations: dropping anchor LS as 3 and anchor RS as 4 or dropping anchor RS as 3 and anchor LS as 4. In the case of dropping anchor LS as 3 and moving to anchor RS, the vessel pulls 3 anchor lines and moves upwind only using the tunnel thrusters.

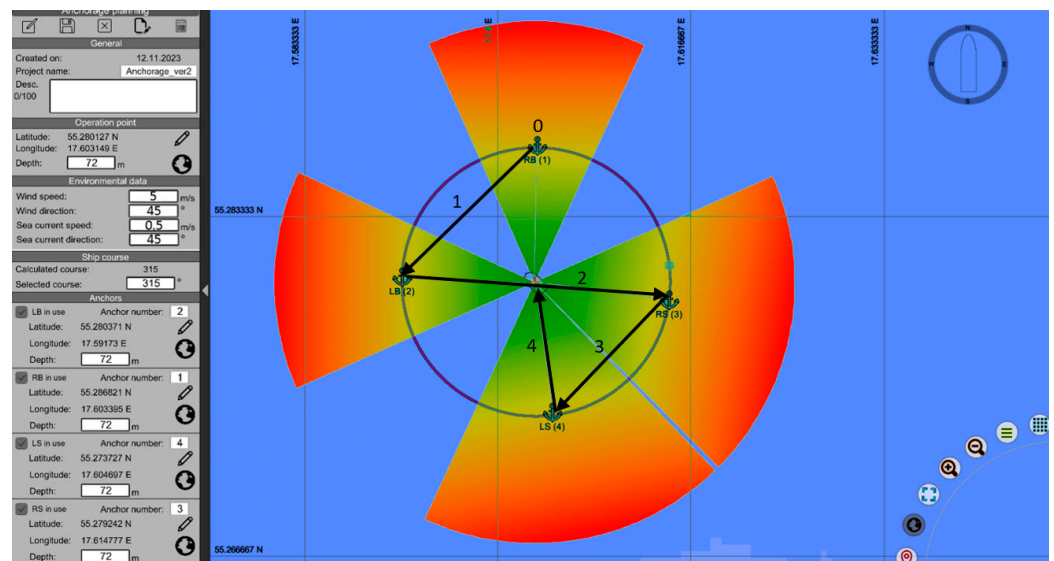


Figure 14. The final arrangement of elements along with the established sequence of anchor drops.

In the case of dropping anchor RS as 3 (arrow 2 in Figure 14) and moving to anchor LS (arrow 3 in Figure 14), also, 3 anchor lines are pulled, but in this case, the vessel moves with the wind. Taking into account environmental conditions and the maneuvering capabilities of the vessel, the algorithm determined the sequence of dropping anchors shown in Figure 14. After deploying all the anchors, the ship should be moved to the operation point using only the anchors (arrow 4 in Figure 14).

While determining the anchor drop sequence, the algorithm, utilizing rules from the cognitive knowledge base, defines all possible paths between the declared points. For each of them, the average energy consumption required for anchor deployment is determined, and then the sequence with the lowest energy consumption is selected. For the navigational scenario presented in Figure 14, information regarding energy consumption is presented in Table 5.

Table 5. Information on energy consumption during anchor deployment.

| Phase | S [NM] | V [knots] | t [h] | Wind Angle [°] | Env. Force Vector (x-Axis; y-Axis) | Sum of Thrust [kN] | Fuel Consumption [l] | Energy Consumption [kWh] |
|----------|--------|-----------|-------|----------------|------------------------------------|--------------------|----------------------|--------------------------|
| RB -> LB | 0.6 | 0.4 | 1.5 | 90 | (0.5 kN; 46 kN) | 137 | 71.61 | 318.66 |
| LB -> RS | 0.84 | 0.4 | 2.1 | 135 | (6 kN; 34 kN) | 152 | 156.89 | 698.16 |
| RS -> LS | 0.6 | 0.4 | 1.5 | 90 | (0.5 kN; 46 kN) | 137 | 71.64 | 318.79 |
| | | | | | | | SUM | 1335.74 |

In Table 5, the following designations were adopted:

- “Phase”—the segment along which the ship is moving;
- “S”—the distance between the specified anchors;
- “V”—the average speed of the ship on a given phase;
- “t”—the time it takes for the ship to traverse a given phase;
- “Wind angle”—the angle of the wind force acting on the ship’s hull;
- “Env. force vector”—The vector of environmental forces acting on the ship;
- “Sum of thrust”—based on information about the interaction of environmental forces and the obtained velocity on a given phase, the algorithm determines the predicted sum of thrusters thrust;
- “Fuel consumption”—based on the thrust force values of each thruster, transit time, and technical data, the algorithm determines the average fuel consumption for a given phase;
- “Energy consumption”—based on the fuel consumption, the algorithm calculates the energy consumed. It is assumed that $1[l] \approx 9.7$ [kWh]. The efficiency of the propulsion system—41 [%].

4. Results

4.1. The Comparison of the Planned Anchor Drop Order for Two Navigation Situations in Unity3D

In the case of anchoring operations, it can happen that the environmental conditions at the operation site differ from those used for anchoring planning. In such a scenario, the operator has the option to plan a new anchoring operation with updated environmental data or recalculate the energy consumption and determine a new sequence for dropping anchors. When determining a new drop sequence, the algorithm compares four possible anchor deployment sequences and proposes the most optimal order with the least energy consumption. Figure 15 depicts a simplified navigation situation from Figure 14 and a new one for which the anchor drop sequence needs to be determined.

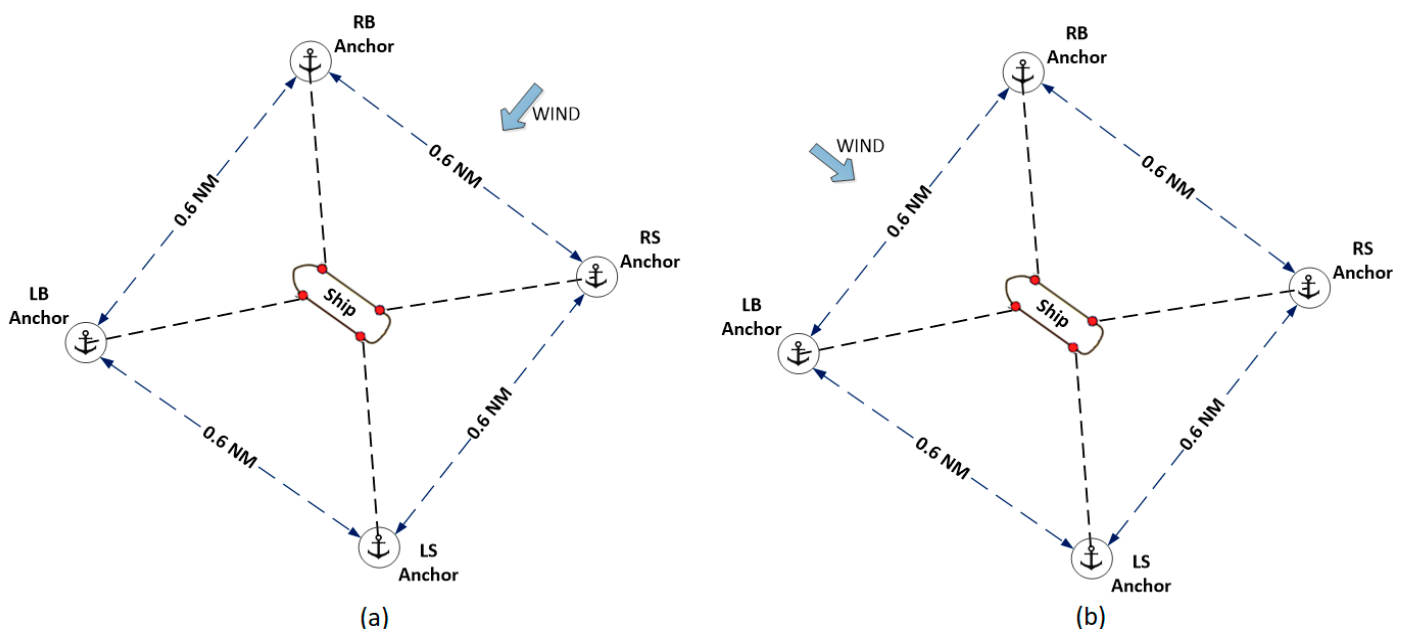


Figure 15. Navigation situation: (a) from Figure 13; (b) new situation.

The above figure shows that the anchor drops points remain unchanged in their positions, but the direction of the wind force on the ship’s hull has changed. The data used to determine the new anchor drop sequence is presented in Table 6.

After analyzing the energy consumption, the algorithm found two anchor deployment scenarios: Case 2 and Case 3 with the total energy consumption about 1369.62 kWh.

Table 6. Results of energy consumption analysis for 4 anchor distribution cases.

| Case | Phase | S [NM] | V [knots] | t [h] | Wind Angle [°] | Env. Force Vector (x-axis; y-axis) | Sum of Thrust [kN] | Fuel Consumption [l] | Energy Consumption [kWh] | |
|------|----------|--------|-----------|-------|----------------|------------------------------------|--------------------|----------------------|--------------------------|--|
| 1 | RB -> LB | 0.6 | 0.4 | 1.5 | 0 | (7.5 kN; 0 kN) | 189 | 110.41 | 446.22 | |
| | LB -> RS | 0.84 | 0.4 | 2.1 | 45 | (5.2 kN; 34 kN) | 138 | 170.88 | 690.62 | |
| | RS -> LS | 0.6 | 0.4 | 1.5 | 0 | (7.5 kN; 0 kN) | 189 | 110.43 | 446.31 | |
| | | SUM | | | | | | | 1538.13 | |
| 2 | RB -> LB | 0.6 | 0.4 | 1.5 | 0 | (7.5 kN; 0 kN) | 189 | 110.41 | 446.24 | |
| | LB -> LS | 0.6 | 0.4 | 1.5 | 0 | (7.5 kN; 0 kN) | 60 | 118.08 | 477.23 | |
| | LS -> RS | 0.6 | 0.4 | 1.5 | 0 | (7.5 kN; 0 kN) | 189 | 110.39 | 446.15 | |
| | | SUM | | | | | | | 1369.62 | |
| 3 | LB -> RB | 0.6 | 0.4 | 1.5 | 0 | (7.5 kN; 0 kN) | 189 | 110.43 | 446.32 | |
| | RB -> RS | 0.6 | 0.4 | 1.5 | 0 | (7.5 kN; 0 kN) | 60 | 118.11 | 477.36 | |
| | RS -> LS | 0.6 | 0.4 | 1.5 | 0 | (7.5 kN; 0 kN) | 189 | 110.42 | 446.26 | |
| | | SUM | | | | | | | 1369.94 | |
| 4 | LB -> RB | 0.6 | 0.4 | 1.5 | 0 | (7.5 kN; 0 kN) | 189 | 110.39 | 446.14 | |
| | RB -> LS | 0.84 | 0.4 | 2.1 | 315 | (5.2 kN; 34 kN) | 138 | 170.91 | 690.76 | |
| | LS -> RS | 0.6 | 0.4 | 1.5 | 0 | (7.5 kN; 0 kN) | 189 | 110.41 | 446.24 | |
| | | SUM | | | | | | | 1583.14 | |

4.2. The Comparison of the Planned Anchor Dropping Sequence in the Anchorage Planning Tool and on the Actual Ship

In Section 3.2, navigation scenarios modeled in Unity3D have been considered to demonstrate the capabilities of the anchor planning tool and the developed cognitive knowledge base. While carrying out research on a real ship, the process of anchor planning and deployment by the ship’s captain was documented using the user interface of the anchor-based positioning system. Figure 16 shows a screenshot of the interface with all anchor-related data.



Figure 16. Screenshot of captain’s anchorage planning.

The user interface from Figure 16 consists of two main sections:

- Left Side: On the left side, all parameters related to the vessel's movement and position are displayed. This section also includes anchor-related data, such as the distance of the anchor from the ship and the length of the anchor line.
- Right Side: On the right side, there are symbols representing the ship and anchors. In the presented scenario in Figure 16, the anchors are shown to be out of range.

Characteristics related to environmental conditions, such as the speed and angle of attack of the wind and sea current on the ship's hull, were also recorded. These were used to reconstruct the environmental conditions during anchorage planning by the algorithm. Figure 17 depicts the relationship between the sea current speed and the operational time.

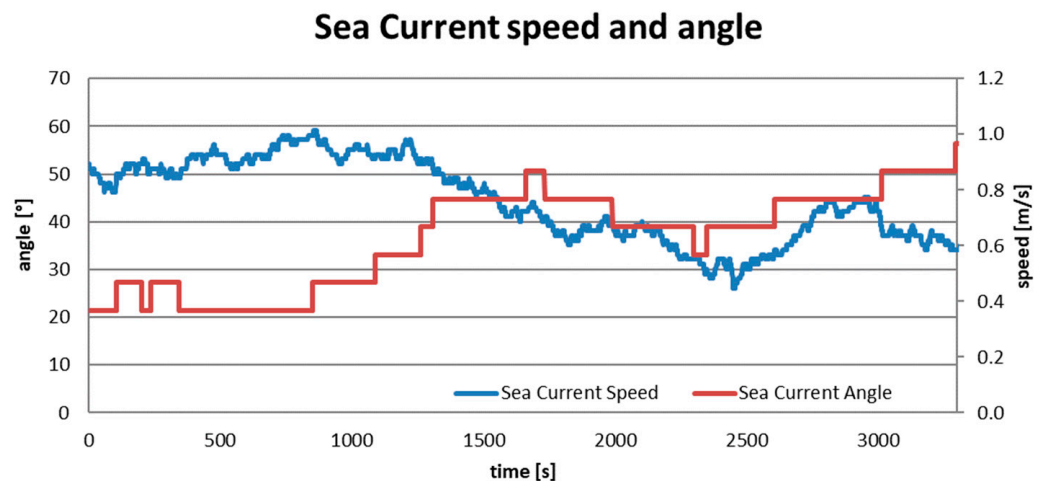


Figure 17. Sea current speed and angle.

Figure 18 depicts the relationship between wind speed and the operational time.

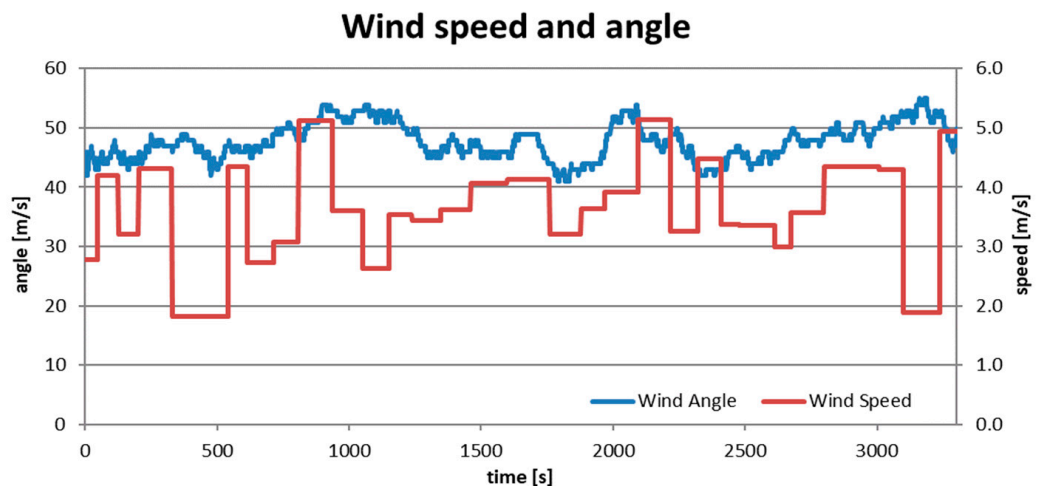


Figure 18. Wind speed and angle.

In Figure 16, it can be observed that individual anchors are not dropped at equal distances from the ship. This uneven distribution may result in poorer position holding during abrupt changes in wind speed. Figure 19 illustrates a simplified diagram of the anchor positions around the ship, along with their respective distances.

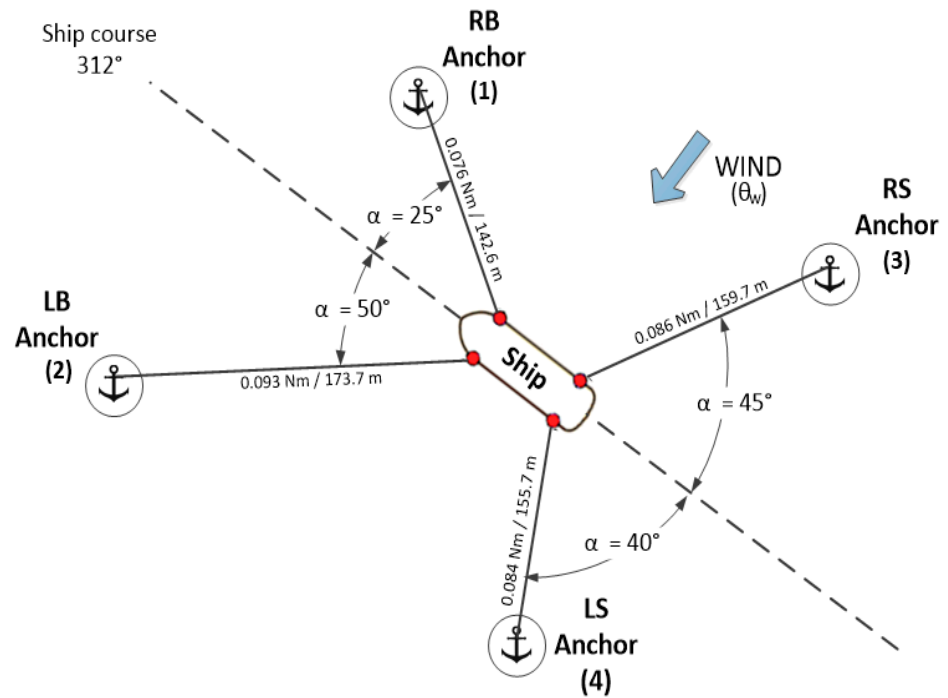


Figure 19. Captain’s anchorage plan.

To compare the anchorage planned by the captain with that generated by the algorithm, a new anchorage was developed in Unity3D incorporating hydrometeorological data extracted from Figures 16–18. Following the sequence outlined in Section 3.2 for anchorage planning, the arrangement of anchors depicted in Figure 20 is obtained.

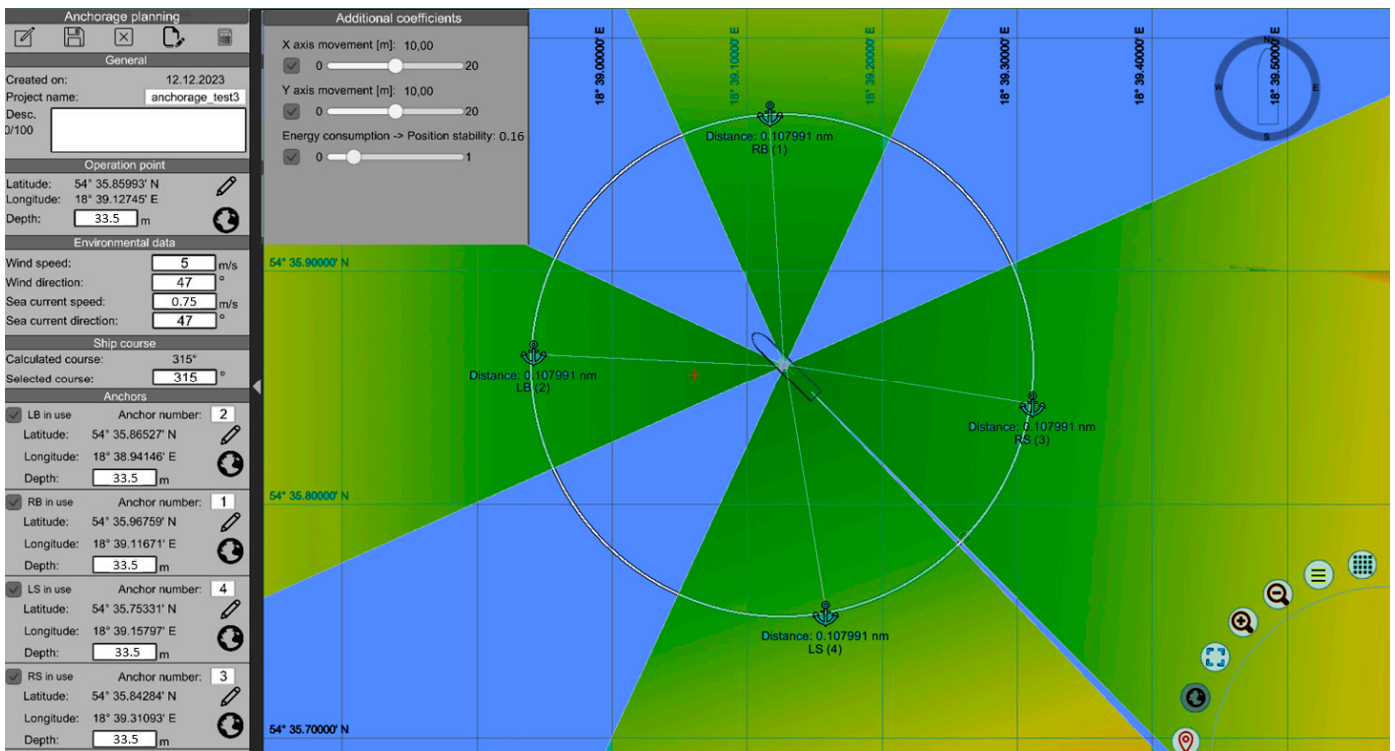


Figure 20. Anchorage arrangements according to the algorithm.

Figure 21 illustrates a simplified diagram of anchorage from Figure 19.

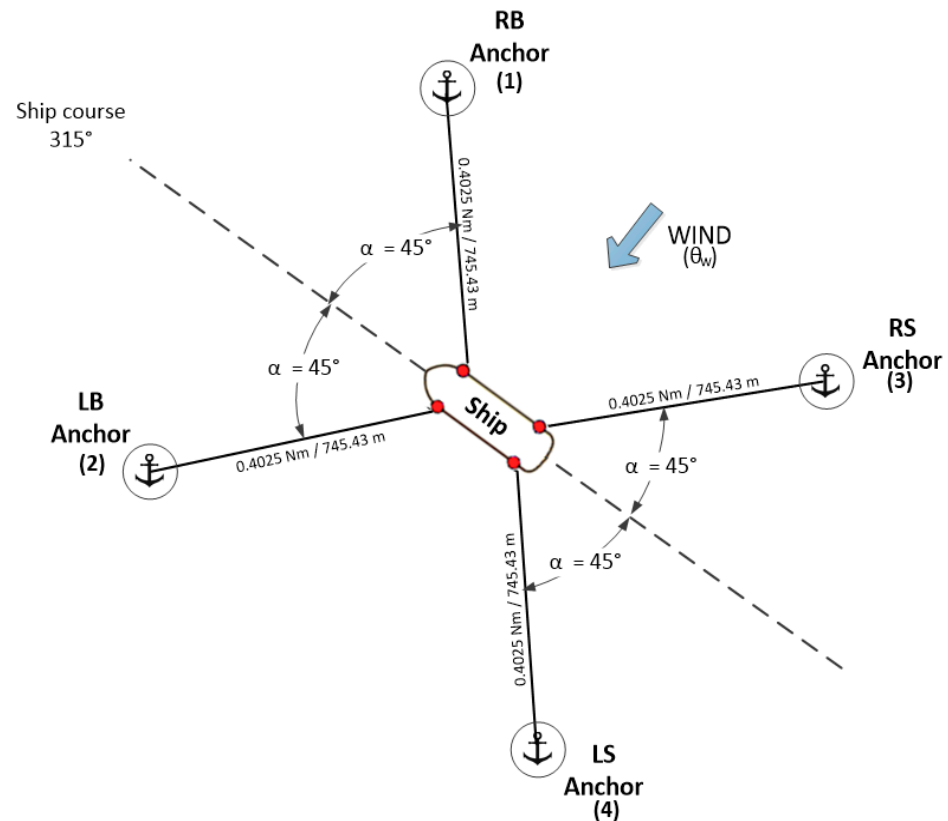


Figure 21. The anchorage plan proposed by the algorithm.

The difference between the two is that the algorithm has determined equal distances to drop anchors from the vessel and deployed them evenly around the vessel. In contrast, the anchors deployed by the captain are at different distances and angles to the vessel.

During anchor planning, the algorithm took into account a stability factor (0.16) that determines the relationship between the stability of holding position and energy consumption. According to this coefficient, it determined the distance of the anchors from the vessel to be approximately 0.1 nautical miles (about 200 m). The master also deployed the anchors at approximately 0.1 nautical miles. Despite the short anchor deployment time and low energy consumption, the close distance of the anchors to the vessel makes the vessel's position less resistant to frequent changes in wind speed. Additionally, with this anchor deployment, the vessel's ability to change its position is limited.

The deployment time of anchors also differs in both cases. According to Table 7, the planned deployment time for anchors determined by the algorithm is 73 min. In the case of anchor deployment by the captain, it took 94 min, but in this case, it took 60 min to prepare the anchorage plan. The total time of the operation was 154 min. The disparity between these two times arises from the fact that the captain had to first plan the entire anchorage.

According to Table 7, the energy consumption for the anchor deployment planned by the captain was 208.87 kWh. For the algorithm, the energy consumption was 196.01 kWh, which is about 8% less consumption compared to the captain's anchor deployment. This is due to the manual control of the individual anchors by the operator. In addition, the anchor arrangement designed by the algorithm was deployment in 52% less time than that deployment by the operator.

Table 7. Results of energy consumption analysis between two anchorage plans. Case 1—Captain’s anchorage plan, Case 2—Anchorage generated by algorithm.

| Case | Phase | S [NM] | V [knots] | t [h] | Wind Angle [°] | Env. Force Vector (x-Axis; y-Axis) | Sum of Thrust [kN] | Fuel Consumption [l] | Energy Consumption [kWh] |
|------|----------|--------|-----------|-------|----------------|------------------------------------|--------------------|----------------------|--------------------------|
| 1 | RB -> LB | 0.09 | 0.29 | 0.31 | 66 | (3 kN; 41 kN) | 74 | 6.75 | 27.28 |
| | LB -> RS | 0.18 | 0.21 | 0.9 | 137 | (5 kN; 33 kN) | 82 | 36.26 | 146.55 |
| | RS -> LS | 0.11 | 0.29 | 0.37 | 92 | (0.5 kN; 48 kN) | 76 | 8.67 | 35.04 |
| | | | | | | | | SUM | 208.87 |
| 2 | RB -> LB | 0.14 | 0.4 | 0.35 | 92 | (0.5 kN; 48 kN) | 76 | 8.48 | 34.27 |
| | LB -> RS | 0.21 | 0.4 | 0.52 | 137 | (5 kN; 33 kN) | 82 | 31.49 | 127.27 |
| | RS -> LS | 0.14 | 0.4 | 0.35 | 92 | (0.5 kN; 48 kN) | 76 | 8.53 | 34.47 |
| | | | | | | | | SUM | 196.01 |

5. Conclusions

The manual process of anchoring planning on ships equipped with an anchoring set typically occurs after reaching the positioning location. The ship’s captain manually draws the anchor deployment phases on the board based on their knowledge and experience. Often, manual planning can take 1 h or more, causing downtime. After drawing the paths between anchor drop points, manual control of the ship follows. The entire anchoring setup, along with planning, can take even 2–3 h. This publication presents a different approach to anchoring planning, using cognitive knowledge. The rules in the knowledge base were developed based on capability plots, research on the real vessel, and the captain’s experience. By utilizing an anchoring planning tool developed in the Unity3D environment, the entire anchoring process can be designed before the ship leaves the port. Additionally, it is possible to export data regarding paths between anchor drop points as individual waypoints and import them into autopilot systems. This significantly reduces the anchoring setup process, resulting in fuel and energy savings.

The navigational scenario presented in Section 3 demonstrates that the process of anchoring planning is highly complex, requiring consideration of various variables related to the maneuvering capabilities of the vessel. It involves introducing coefficients that determine, for example, the positioning goal—whether the ship should remain stationary or have the ability to change the set point. All these variables make it impossible to consider all possible scenarios in a single publication.

At the end of Section 3, a comparison was presented between the anchoring plan devised by the ship’s captain and the anchoring plan generated by the algorithm. The algorithm effectively reduced the anchoring time by approximately 52%, despite the anchors being positioned farther from the ship. Energy consumption was also lower for the anchorage planned by the algorithm about 8%.

Author Contributions: Conceptualization, J.W. and A.L.; computations, J.W. and A.L.; methodology, J.W. and A.L.; experimental verification, J.W. and A.L.; writing text of the article, J.W. and A.L.; review and editing, J.W. and A.L.; visualization, J.W. and A.L.; supervision, J.W. and A.L. All authors have read and agreed to the published version of the manuscript.

Funding: This research was funded by the research project “Control of formation of vessels with low-emission propulsion” No. WE/2023/PZ/08, Electrical Engineering Faculty, Gdynia Maritime University, Poland.

Data Availability Statement: The data from this study can be provided upon request to the corresponding author. They are not publicly accessible owing to privacy concerns.

Conflicts of Interest: The authors declare no conflicts of interest.

References

1. Chin, C.S.; Lio, C.S. Sliding-Mode Control of STENA DRILLMAX Drillship with Environmental Disturbances for Dynamic Positioning. In *Proceedings of the 11th International Conference on Modelling, Identification and Control (ICMIC2019)*; Wang, R., Chen, Z., Zhang, W., Zhu, Q., Eds.; Springer: Singapore, 2020; pp. 99–111. ISBN 978-981-15-0473-0.
2. Machado, L.d.V.; Fernandes, A.C. Moonpool dimensions and position optimization with Genetic Algorithm of a drillship in random seas. *Ocean. Eng.* **2022**, *247*, 110561. [[CrossRef](#)]
3. Bruschi, R.; Vitali, L.; Marchionni, L.; Parrella, A.; Mancini, A. Pipe technology and installation equipment for frontier deep water projects. *Ocean. Eng.* **2015**, *108*, 369–392. [[CrossRef](#)]
4. International Conference on Ocean. *ASME 2009 28th International Conference on Ocean, Offshore and Arctic Engineering. May 31–June 5, 2009, Honolulu, Hawaii, USA. Volume 3, Pipeline and Riser Technology*; ASME: New York, NY, USA, 2009; ISBN 978-0-7918-4343-7.
5. Yu, W.; Duan, C.; Kuang, C.; Zhang, H.; Wu, P.; Dai, W. Offshore towed-streamer positioning based on variance component estimation. *Ocean. Eng.* **2023**, *278*, 114355. [[CrossRef](#)]
6. Wartsila. Offshore Support Vessels (OSVs). Available online: <https://www.wartsila.com/encyclopedia/term/offshore-support-vessels-osvs> (accessed on 4 November 2023).
7. Chellapurath, M.; Walker, K.L.; Donato, E.; Picardi, G.; Stefanni, S.; Laschi, C.; Giorgio-Serchi, F.; Calisti, M. Analysis of Station Keeping Performance of an Underwater Legged Robot. *IEEE/ASME Trans. Mechatron.* **2022**, *27*, 3730–3741. [[CrossRef](#)]
8. Peng, Z.; Wang, J.; Wang, D.; Han, Q.-L. An Overview of Recent Advances in Coordinated Control of Multiple Autonomous Surface Vehicles. *IEEE Trans. Ind. Inf.* **2021**, *17*, 732–745. [[CrossRef](#)]
9. Wang, Y.; Wang, H.; Li, M.; Wang, D.; Fu, M. Adaptive fuzzy controller design for dynamic positioning ship integrating prescribed performance. *Ocean. Eng.* **2021**, *219*, 107956. [[CrossRef](#)]
10. Haseltalab, A.; Negenborn, R.R. Model predictive maneuvering control and energy management for all-electric autonomous ships. *Appl. Energy* **2019**, *251*, 113308. [[CrossRef](#)]
11. Walker, K.L.; Stokes, A.A.; Kiprakis, A.; Giorgio-Serchi, F. Impact of Thruster Dynamics on the Feasibility of ROV Station Keeping in Waves. In *Proceedings of the Global Oceans 2020: Singapore—U.S. Gulf Coast, Biloxi, MS, USA, 5–30 October 2020*; pp. 1–7. ISBN 978-1-7281-5446-6.
12. Lisowski, J. Optimality of Safe Game and Non-Game Control of Marine Objects. *Electronics* **2023**, *12*, 3637. [[CrossRef](#)]
13. Koznowski, W.; Kula, K.; Lazarowska, A.; Lisowski, J.; Miller, A.; Rak, A.; Rybczak, M.; Mohamed-Seghir, M.; Tomera, M. Research on Synthesis of Multi-Layer Intelligent System for Optimal and Safe Control of Marine Autonomous Object. *Electronics* **2023**, *12*, 3299. [[CrossRef](#)]
14. Mohamed-Seghir, M.; Kula, K.; Kouzou, A. Artificial Intelligence-Based Methods for Decision Support to Avoid Collisions at Sea. *Electronics* **2021**, *10*, 2360. [[CrossRef](#)]
15. Kaizer, A.; Winiarska, M.; Formela, K.; Neumann, T. Inland Navigation as an Opportunity to Increase the Cargo Capacity of the Tri-City Seaports. *Water* **2022**, *14*, 2482. [[CrossRef](#)]
16. Guze, S.; Smolarek, L.; Weintrit, A. The area-dynamic approach to the assessment of the risks of ship collision in the restricted water. *Sci. J. Marit. Univ. Szczec.* **2016**, *117*, 88–93. [[CrossRef](#)]
17. Weintrit, A. Initial Description of Pilotage and Tug Services in the Context of e-Navigation. *JMSE* **2020**, *8*, 116. [[CrossRef](#)]
18. Weintrit, A. Clarification, Systematization and General Classification of Electronic Chart Systems and Electronic Navigational Charts Used in Marine Navigation. Part 2—Electronic Navigational Charts. *TransNav* **2018**, *12*, 769–780. [[CrossRef](#)]
19. Rak, A.; Miller, A. Modelling of Lake Waves to Simulate Environmental Disturbance to a Scale Ship Model. *Pol. Marit. Res.* **2023**, *30*, 12–21. [[CrossRef](#)]
20. Rybczak, M.; Gierusz, W. Maritime Autonomous Surface Ships in Use with LMI and Overriding Trajectory Controller. *Appl. Sci.* **2022**, *12*, 9927. [[CrossRef](#)]
21. Soliwoda, J.; Kaizer, A.; Neumann, T. Possibility of Capsizing of a Dredger during Towing. *Water* **2021**, *13*, 3027. [[CrossRef](#)]
22. Madadi, B.; Aksakalli, V. A stochastic approximation approach to spatio-temporal anchorage planning with multiple objectives. *Expert Syst. Appl.* **2020**, *146*, 113170. [[CrossRef](#)]
23. Oz, D.; Aksakalli, V.; Alkaya, A.F.; Aydogdu, V. An anchorage planning strategy with safety and utilization considerations. *Comput. Oper. Res.* **2015**, *62*, 12–22. [[CrossRef](#)]
24. Jajac, N.; Kilić, J.; Rogulj, K. An Integral Approach to Sustainable Decision-Making within Maritime Spatial Planning—A DSC for the Planning of Anchorages on the Island of Šolta, Croatia. *Sustainability* **2019**, *11*, 104. [[CrossRef](#)]
25. Abramowicz-Gerigk, T.; Burciu, Z.; Jaworski, T.; Nowicki, J. The Large-Scale Physical Model Tests of the Passing Ship Effect on a Ship Moored at the Solid-Type Berth. *Sensors* **2022**, *22*, 868. [[CrossRef](#)] [[PubMed](#)]
26. Przybylowski, A.; Suchanek, M.; Miszewski, P. COVID-19 Pandemic Impact on a Global Liner Shipping Company Employee Work Digitalization. *TransNav* **2022**, *16*, 759–765. [[CrossRef](#)]
27. Dang, X.-K.; Do, V.-D.; Nguyen, X.-P. Robust Adaptive Fuzzy Control Using Genetic Algorithm for Dynamic Positioning System. *IEEE Access* **2020**, *8*, 222077–222092. [[CrossRef](#)]
28. Fossen, T.I. *Handbook of Marine Craft Hydrodynamics and Motion Control*; Wiley: Hoboken, NJ, USA, 2011.
29. Walker, K.L.; Gabl, R.; Aracri, S.; Cao, Y.; Stokes, A.A.; Kiprakis, A.; Giorgio-Serchi, F. Experimental Validation of Wave Induced Disturbances for Predictive Station Keeping of a Remotely Operated Vehicle. *IEEE Robot. Autom. Lett.* **2021**, *6*, 5421–5428. [[CrossRef](#)]

30. Robert Stewart. Ocean-Wave Spectra. Available online: https://wikiwaves.org/Ocean-Wave_Spectra (accessed on 5 November 2023).
31. DNV. Main Website. Available online: <https://www.dnv.com/index.html> (accessed on 5 November 2023).
32. DNV Rules and Standards. Assessment of Station Keeping Capability of Dynamic Positioning Vessels. Available online: <https://standards.dnv.com/explorer/document/7E231C260D4846DF8DF3CBA12A2229D4/5> (accessed on 12 December 2023).

Disclaimer/Publisher's Note: The statements, opinions and data contained in all publications are solely those of the individual author(s) and contributor(s) and not of MDPI and/or the editor(s). MDPI and/or the editor(s) disclaim responsibility for any injury to people or property resulting from any ideas, methods, instructions or products referred to in the content.